OMÜ Mühendislik Bilimleri ve Teknolojisi Dergisi,
OMU Journal of Engineering Sciences and Technology
e-ISSN: 2791-8858 OMUJEST, 2026, 7: 90-104

Usage of the *g* Control Chart in Monitoring Rare Events: An Analysis of Earthquake Data

Nadir Olayların İncelenmesinde *g* Kontrol Grafiğini Kullanımı: Deprem Verisinin Analizi

Gülsüm Sıla ERGÜVEN[1], Sermin ELEVLİ[2]

[1] Department of Industrial Engineering, Ondokuz Mayıs University, Samsun, Türkiye
• **erguven.sila.gulsum@gmail.com** • ORCID > 0009-0007-9133-6907

[2] Department of Industrial Engineering, Ondokuz Mayıs University, Samsun, Türkiye
• **sermin.elevli@omu.edu.tr** • ORCID > 0000-0002-7712-5536

Makale Bilgisi/Article Information

Makale Türü/Article Type: Araştırma Makalesi/Research Article
Geliş Tarihi/Received: 16 Temmuz/July 2026
Kabul Tarihi/Accepted: 14 Eylül/September 2026
Yıl/Year: 2026 | **Cilt/Volume:** 7 | **Sayfa/Pages:** 90-104

Atıf/Cite as: Ergüven, G.S., Elevli, S. "Usage of the *g* Control Chart in Monitoring Rare Events: An Analysis of Earthquake Data" OMU Journal of Engineering Sciences and Technology, 7, 2026: 90-104.

Sorumlu Yazar/Corresponding Author: Prof. Dr. Sermin ELEVLİ

USAGE OF THE G CONTROL CHART IN MONITORING RARE EVENTS: AN ANALYSIS OF EARTHQUAKE DATA

ABSTRACT

Rare events are events that, although occurring infrequently, can have significant consequences and are often difficult to monitor using traditional statistical process control tools. Especially in processes with low event counts, frequent zero observations, and irregular event intervals, traditional control charts may have limited sensitivity. This study examines the geometric distribution-based *g* control chart for monitoring rare events and evaluates its applicability to earthquake data. In the application, earthquake data covering the 1995–2025 period for the provinces of Amasya, Çorum, and Tokat in the TR83 Level 2 Region were used, and earthquakes with magnitude Mx ≥ 4.0 were considered rare events. At the provincial level, *g* control charts were constructed using the observation intervals between events, and unusual changes in seismic activity were analysed. The findings showed that narrower control limits generated more frequent signals, whereas wider control limits produced fewer signals and a lower nominal in-control signalling probability. However, because no independent validation criterion was available, these signals were not directly classified as false alarms or as physically meaningful seismic anomalies. Overall, the study demonstrates that the *g* control chart can serve as a complementary statistical monitoring tool not only in industrial and service processes but also for rare, high-impact natural events such as earthquakes.

Keywords: Rare Events, *g* Control Chart, Earthquake Magnitude

❄ ❄ ❄

NADİR OLAYLARIN İNCELENMESİNDE G KONTROL GRAFİĞİNİ KULLANIMI: DEPREM VERİSİNİN ANALİZİ

ÖZET

Nadir olaylar, seyrek meydana gelmelerine rağmen önemli sonuçlar doğurabilen olaylar olup, bu olayların geleneksel istatistiksel süreç kontrol araçlarıyla izlenmesi çoğu zaman güçtür. Özellikle olay sayısının düşük, sıfır gözlemlerin sık ve olaylar arasındaki zaman aralıklarının düzensiz olduğu süreçlerde, geleneksel kontrol grafikleri yeterli duyarlılığa sahip değildir. Bu çalışmada, nadir olayların izlenmesinde kullanılan geometrik dağılıma dayalı *g* kontrol grafiği ele alınmış ve deprem verilerine uygulanabilirliği incelenmiştir.

Uygulamada, TR83 Düzey 2 Bölgesi'nde yer alan Amasya, Çorum ve Tokat illerine ait 1995–2025 dönemini kapsayan deprem verileri kullanılmış ve büyüklüğü Mx ≥ 4.0 olan depremler nadir olaylar olarak ele alınmıştır. Olaylar arasındaki gözlem aralıkları kullanılarak il bazında *g* kontrol grafikleri oluşturulmuş ve sismik aktivitedeki olağan dışı hareketler analiz edilmiştir. Bulgular, dar kontrol sınırlarının daha sık sinyal ürettiğini, daha geniş kontrol sınırlarının ise daha az sinyal ve daha düşük nominal kontrol-içi sinyal olasılığı ile sonuçlandığını göstermiştir. Bununla birlikte, bağımsız bir doğrulama ölçütü bulunmadığından, bu sinyaller doğrudan yanlış alarm veya fiziksel olarak anlamlı sismik anomaliler olarak sınıflandırılmamıştır. Sonuç olarak çalışma, *g* kontrol grafiğinin yalnızca endüstriyel ve hizmet süreçlerinde değil, deprem gibi nadir görülen ancak etkisi yüksek doğal olayların izlenmesinde de destekleyici bir istatistiksel araç olduğunu ortaya koymaktadır.

Anahtar Kelimeler: Nadir Olaylar, *g* Kontrol Grafiği, Deprem Büyüklüğü

Highlights

- The *g* control chart was successfully adapted for monitoring rare earthquakes.
- Seismic activity in Amasya, Corum, and Tokat was examined.
- The study extends statistical process control to disaster management.

❋ ❋ ❋

1. INTRODUCTION

Control charts, one of the principal tools of Statistical Process Control (SPC), are widely used to monitor process variability over time and to detect deviations. Among the basic assumptions for effective process monitoring with traditional control charts are that events occur with sufficient frequency and that the dataset does not contain an excessive number of zero observations. Rare events, on the other hand, occur with low probability and infrequently but may have significant consequences. Such events occur in many fields, including healthcare, manufacturing, safety, transportation, and natural disasters. The main characteristic of rare events is that they challenge assumptions underlying traditional control-chart approaches, particularly those based on the mean and variance. In particular, a very low number of events, a high frequency of zero observations, and irregular event intervals may render traditional control charts insufficiently sensitive to such data [1-3]. Therefore, effective monitoring of rare

events and the detection of potential process changes have become a distinct area of study within SPC.

Various control charts are used in SPC to evaluate process performance and monitor process changes. Traditional Shewhart-type control charts, such as the p, np, c, and u control charts, generally yield effective results when events are observed more frequently and when the number of defects or nonconformities per unit is sufficiently large. However, in processes involving rare events, these charts are often inadequate. This is because, in such processes, no events may be observed for a long period, and variability may show more in the waiting time between events or in the number of observations, rather than in the number of events themselves. In this context, special control charts, such as the g and t control charts, have been developed to monitor rare events, based on the time or number of units between events [4, 5].

A review of the literature indicates that g control charts are effective statistical tools for monitoring and analysing events with a low probability of occurrence. Kaminsky et al. [1] established the theoretical basis of the g control chart within a geometric-distribution framework and developed an important statistical monitoring approach for rare events. Benneyan et al. [6] examined the use of statistical process control in healthcare and emphasized the role of control charts in distinguishing changes in process performance from natural variability, particularly when rare but critical events are monitored.

Park and Wang [7] reconsidered *g* control charts and evaluated estimators for cases in which the process parameter is unknown, noting in particular that the minimum-variance unbiased estimator has been used inappropriately in the quality engineering literature. The same study also proposed an alternative setup approach for unbalanced sample structures. These findings demonstrate the important role of parameter estimation and sample structure in the performance of the *g* control chart.

Application-based studies also support the interpretability and practical utility of the *g* control chart in areas where rare but critical events are monitored. Alexander [8] examined *g* and *t* control charts for monitoring rare events and demonstrated their use with healthcare data. Such recent applications confirm that the g control chart is useful not only at the theoretical level but also for monitoring real-world processes.

Among the most important natural disasters, earthquakes can also be considered rare but high-impact events when evaluated against certain magnitude thresholds [9, 10]. Within this framework, examining not only the numerical

frequencies of earthquakes but also the time intervals, or opportunities, between successive significant earthquakes provides meaningful information for understanding seismic processes. The *g* control chart, which is based on the number of observations between two events, is a useful method for statistically monitoring the increasing or decreasing frequency of seismic activity across observation units between earthquakes of a certain magnitude [11, 12]. Energy accumulates along fault lines due to tectonic movements, and small-scale earthquakes may not always fully release it. Under certain conditions, this may indicate stress accumulation. However, it is also known that not every long period of seismic silence results in a major earthquake [13]. Therefore, rather than being a tool that directly predicts earthquakes, the g control chart makes statistical deviations in earthquake frequency above certain thresholds visible, thereby enabling geoscientists to monitor unusual changes in seismic activity. In particular, the tendency of earthquakes in a given region to cluster or to exhibit unexpected stability may contribute to the development of new scientific hypotheses regarding stress accumulation, energy release, or interactions between fault segments. Thus, although such signals do not directly yield a prediction, they may help support precautionary assessments by indicating possible changes in risk levels.

This study aims to apply the g control chart, which is used for monitoring rare events, to earthquake data. Focusing on the intervals between earthquakes rather than solely on their frequency provides a different perspective on the temporal structure of seismic activity. Furthermore, comparing alternative control-limit settings allows the effect of limit width on signal frequency to be evaluated without presuming that individual signals are either false alarms or physically meaningful anomalies. In this respect, the study presents an interdisciplinary application of statistical process control techniques and demonstrates their potential use beyond industrial processes for the statistical monitoring of rare natural events. In contrast to Taskin and Masud [9], who focused on identifying and analysing unusual earthquake frequencies using statistical control charts, this study examines the number of opportunities between consecutive earthquakes with magnitude $Mx \geq 4.0$ using the g control chart. In addition, the effects of alternative control-limit settings on the number of out-of-control signals are assessed.

2. MATERIALS AND METHODS

2.1. Rare Events and *g* Control Charts

An event is any observable situation, change, or occurrence that takes place at a specific time and location. As a situational concept, an event can also be defined as the change of an object's property from one state or level to another. Rare events,

on the other hand, are those with a low probability of occurrence but that may lead to significant consequences when they do occur. Rare events are generally monitored by the number of conforming events (or opportunities) between successive rare events. Figure 1 shows conforming events/opportunities (such as failure-free operation of a machine, production of defect-free parts, or uninterrupted service of an electrical system), rare events (such as floods, large-scale earthquakes, occupational accidents involving injuries, or war), and the number of conforming events occurring between two successive rare events.

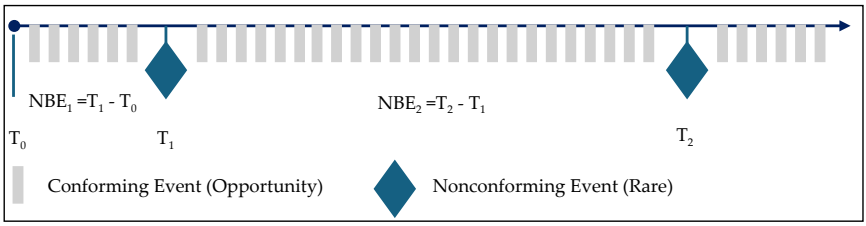


Figure 1. Number of conforming events between successive rare events.

The *g* control chart is one of the SPC tools commonly considered for monitoring rare events. When the adverse events of interest are rare, this type of control chart serves as an alternative to standard attribute control charts, with control limits calculated using geometric distribution. The tendency of events in the process to occur more or less frequently can be monitored by tracking systematic changes in the number of observations between events.

For the *g* chart, the event probability p is estimated as follows:

$$p = \frac{(N - 1) / N}{\bar{x} + 1} \tag{1}$$

where N is the number of data values used in the calculations and $\bar{x}$ is the mean of the points plotted on the chart.

The theoretical structure of the g chart is based on the geometric distribution [1, 14]. Accordingly, the probability mass function of the random variable is given as:

$$P(X = x) = p\,(1 - p)^{x - a} \qquad x = a, a+1, \ldots \tag{2}$$

where X is the number of observations between events, p is the probability of event occurrence, and a is the smallest value that the variable can take.

In discrete-time event monitoring processes, the observed variable can be defined in two ways. In the number-between approach, the variable represents the number of event-free units between two consecutive events. In this case, the unit in which the event occurs is excluded from the count. Therefore, if two events occur consecutively, there is no event-free unit between them, and the observation takes the value $a = 0$. In contrast, in the number-until approach, the variable represents the total number of units observed until an event occurs. In this definition, the unit in which the event occurs is also included in the count. Therefore, if the event occurs in the first unit, the observed value is 1, and $a = 1$ is used. In brief, if the process is monitored based on the number of event-free units between two consecutive events (number between), $a = 0$ is used; whereas if it is monitored based on the number of units counted until an event occurs (number until), $a = 1$ is used [14].

In the classical approach, the centerline and control limits for the g control chart can be constructed based on the mean and variance. However, due to the right-skewed nature of the geometric distribution, probability-based limits are more commonly preferred [1]. The centerline is based on the median (50th percentile), while the control limits are based on selected percentiles of the geometric distribution. Additionally, the calculation uses the definition "up to a number," and the graph shows values "between a number." One is subtracted from the resulting geometric quantile. In this study, probability-based control limits were used. For Test 1, the k value is related to the percentile limits via the standard normal cumulative distribution function: the lower tail probability is $\Phi(-k)$, and the upper percentile is $\Phi(k)$. Thus, $k = 1$ corresponds approximately to percentiles 0.1587 and 0.8413, while $k = 3$ corresponds approximately to percentiles 0.00135 and 0.99865. These probability values are converted into g control chart limits using the inverse cumulative distribution function of the geometric distribution [15]. Accordingly, the lower control limit, midline, and upper control limit for the g control chart are calculated as follows;

$$LCL' = \left[\frac{ln(1-\alpha_{LCL})}{ln(1-p)} + a\right]^{-} \tag{3}$$

$$CL' = \left[\frac{ln(0.5)}{ln(1-p)} + a\right]^{-} \tag{4}$$

$$UCL' = \left[\frac{ln(\alpha_{UCL})}{ln(1-p)} + a - 1\right]^{+} \tag{5}$$

where *LCL'* is the lower control limit, *CL'* is the center line, *UCL'* is the upper control, p is the probability of an event occurring, α_{UCL} is the tail probability selected for the upper control limit, α_{LCL} is the tail probability selected for the lower control limit, and $ln(\cdot)$ is the natural logarithm function. The expression $[]^+$ indicates that the result is rounded up, whereas $[]^-$ indicates that the result is rounded down [10].

In this chart, special-cause tests can be used in addition to the basic assessment of points relative to the control limits. The Benneyan test is particularly relevant to g charts because it evaluates runs of consecutive points at the lower control limit, which may occur when rare events become unusually frequent. The required run length depends on the probability of a point being at the lower limit and on the selected k value. The formulation used for this test follows Benneyan [14], and Equation (6) presents the corresponding principle.

$$cp = \frac{ln(\text{CDF}(-k))}{ln(p)} \tag{6}$$

where cp is the number of consecutive points that must be equal to the lower control limit, p is the probability that a point is equal to the lower control limit and k is the coefficient indicating how many standard deviations away from the center line the control limit is established. CDF stands for "cumulative distribution function." The expression CDF($-k$) indicates the probability to the left of $-k$ in the standard normal distribution.

One commonly used measure for evaluating the performance of the *g*-chart is the ARL (Average Run Length) concept [16, 17]. ARL refers to the average number of observations that occur until the control chart gives a signal. In the simple single-signal approach, the expected number of observations until a false alarm when the process is in control is denoted by ARL_0, whereas the expected number of observations until a signal after the process goes out of control is denoted by ARL_1.

$$ARL_0 = \frac{1}{\alpha} \tag{7}$$

$$\alpha = P(X < LCL) + P(X > UCL) \tag{8}$$

where α is the probability of giving a signal when the process is actually in control (Type I error probability). Accordingly, as α decreases, the frequency of false alarms decreases and ARL_0 increases.

2.2. Earthquake Data

Earthquakes above a certain threshold value can also be evaluated within the rare-event approach. In particular, since earthquakes in a selected region are infrequent but high-impact events, both their numerical frequency and the intervals between successive events are important. Therefore, control charts developed to monitor rare events provide a suitable basis for evaluating earthquake data from a statistical process monitoring perspective. Accordingly, earthquakes that occurred in the TR83 region have been included in the analysis in this study. The TR83 region was chosen because it offers a geographically integrated study area encompassing provinces exposed to the North Anatolian Fault Zone (NAFZ) at varying levels, and allows for the comparison of time intervals between earthquake events on a province-by-province basis.

The TR83 Level 2 Region, encompassing the provinces of Amasya, Çorum, Samsun, and Tokat, is a geologically and seismically active area. The southern boundary of the region is defined by NAFZ, a right-lateral strike-slip fault approximately 1200 km long. The NAFZ is known as one of Turkey's most active and prominent fault systems, and therefore carries a high seismic hazard potential. The provinces of Tokat and Amasya are directly affected by this main fault zone. The provinces of Samsun and Çorum are under the influence of both this main zone and secondary fault segments in the region. This indicates that the region has a multi-source seismic risk structure. Figure 2 shows a visual representation of the fault obtained using the MTA Geosciences Map Viewer [18].

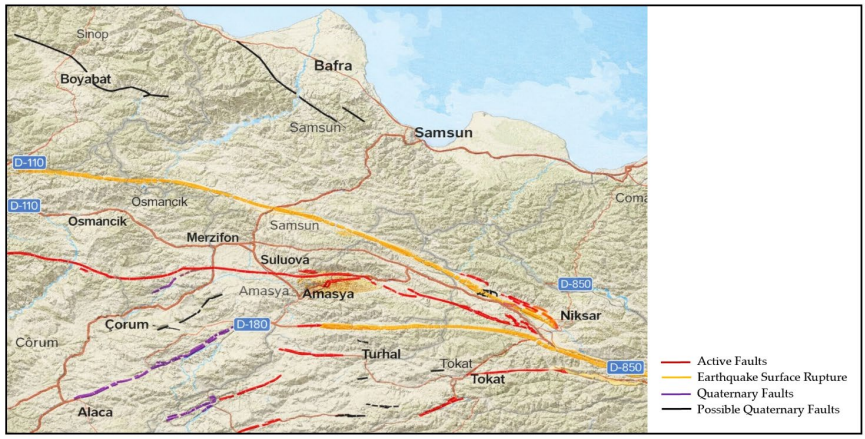


Figure 2. Fault map of the TR83 Level 2 region.

Earthquakes, which are the shaking of the ground surface and the media through which sudden vibrations caused by ruptures within the Earth's crust propagate in the form of waves, are classified according to the measure of the energy released at the earthquake source, namely their magnitude. Earthquake magnitude classification is a seismological classification based on the amount of energy released and is presented in Table 1 [19].

Table 1. Earthquake magnitude classification.

Earthquake Magnitude	Classification	Average Effects
≥8.0	Great	Complete destruction over wide areas, severe damage.
7.0 - 7.9	Major	Serious damage, severe destruction of buildings, and risk of loss of life.
6.0 - 6.9	Strong	Damaging effects in densely populated areas.
5.0 - 5.9	Moderate	Damage to vulnerable structures; felt by everyone.
4.0 - 4.9	Light	Objects shake, clearly felt, damage is rare.
3.0 - 3.9	Minor	Often felt but does not cause damage.
≤2.9	Micro	Usually not felt, recorded only by instruments.

The seismic data used in this study were obtained from the databases of Boğaziçi University Kandilli Observatory and Earthquake Research Institute (KOERI) and the Regional Earthquake-Tsunami Monitoring and Evaluation Center (RETMC), covering the period 1995–2025. Earthquakes with magnitude Mx ≥ 4.0 were included in the analysis. During the relevant period, the number of earthquakes recorded in Amasya, Çorum, and Tokat provinces with a magnitude of Mx ≥ 4.0 were 26, 25, and 24, respectively. These earthquake numbers correspond to 25, 24, and 23 consecutive time intervals, as the number of consecutive events is one less than the number of events themselves. In this application, an "opportunity" is defined as a calendar day between two consecutive Mx ≥ 4.0 earthquakes. Accordingly, the "number-between" value is 0 for two earthquakes occurring on the same calendar day. The average number of opportunities between events was calculated as 425.92 days for Amasya, 417.04 days for Çorum, and 456.04 days for Tokat. The probability of an event was estimated from the data using the formula according to the number-between geometric model. Accordingly, $p = 0.002342$ was obtained for Amasya, $p = 0.002392$ for Çorum, and $p = 0.002188$ for Tokat. Since the p-value is shown with three decimal places in the graph title, all three estimates appear as $p = 0.002$. Therefore, the 0.002 value was not predetermined as a common and fixed

probability for the three provinces. It was calculated separately for each province using the formula. No seismological declustering was applied to the earthquake catalog. Therefore, aftershocks and other temporally dependent earthquake sequences included in the source catalog were preserved in the analysis. Short inter-event intervals and clustering-related graph signals should be considered when interpreting the data. The presence of dependent earthquake sequences may weaken the interpretation of the geometric model's independence assumption. Earthquakes of magnitude 4.0 and above are recorded more reliably than lower magnitude earthquakes and represent more significant seismic events. They were chosen because they reduce noise in the analysis. Samsun province was excluded from the analysis because no earthquakes of magnitude 4.0 and above were observed during the relevant period. Therefore, the 4.0 earthquake magnitude threshold should not be considered the sole and absolute most suitable seismic threshold, but rather an operational threshold selected for this study. A sensitivity analysis for alternative threshold values such as 3.5, 4.5, or 5.0 was not performed in the current analysis.

3. RESULTS

The *g* control charts were constructed for Amasya, Çorum, and Tokat using the number-between values expressed in calendar days (Figure 3). The Mx ≥ 4.0 earthquakes were arranged chronologically, and the day count between each pair of successive events was used as the plotted variable. Separate control charts were created based on different k values. Here, k represents the width of the probability-based control limits from the centerline.

The exact event-probability estimates differ slightly by province (Amasya: 0.002342; Çorum: 0.002392; Tokat: 0.002188), although each is displayed as 0.002 after rounding in Figure 3. Using the control limits shown in the charts, the numbers of plotted points outside the control limits were 23 for Amasya, 17 for Çorum, and 12 for Tokat when $k = 1$; for $k = 3$, one point was outside the control limits in each province. These counts refer specifically to points below the LCL or above the UCL and are separate from additional run-rule or Benneyan-test indications. The larger number of outside-limit points at $k = 1$ reflects the narrower percentile limits. However, these signals should not automatically be interpreted as false alarms without an independent validation criterion. Likewise, the fewer $k = 3$ signals should be interpreted as statistical indications of unusual event spacing rather than as direct evidence of physical clustering, non-stationarity, stress transfer, or triggering.

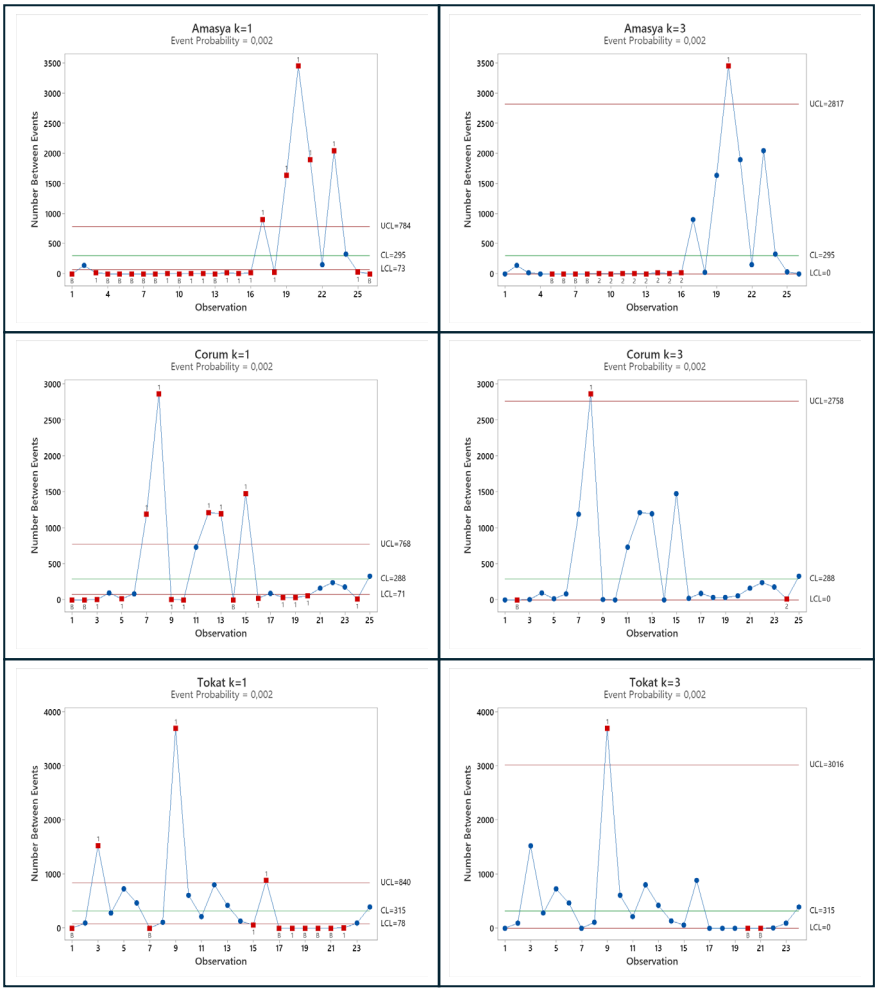


Figure 3. *g* control charts by city.

Upon examining the charts, signal generation was more frequent for $k = 1$ because of the narrower control limits, whereas the wider $k = 3$ limits produced fewer signals. To support this visual assessment numerically, the corresponding ARL0 values were calculated and are presented in Table 2.

Table 2. Calculated ARL_0 Values.

	AMASYA		ÇORUM		TOKAT	
	$k = 1$	$k = 3$	$k = 1$	$k = 3$	$k = 1$	$k = 3$
ARL_0	2,9	281,93	2,8	250,52	3,0	419,91

Table 2 shows that the ARL_0 values obtained for $k = 1$ are lower than those obtained for $k = 3$ in all three provinces. The reported ARL_0 values were calculated analytically using Equation (7) and (8), and they were not obtained from simulation or from the observed empirical signal frequency. For $k = 3$, the estimated event probability for Tokat ($p = 0.002188$) is lower than those for Amasya ($p = 0.002342$) and Çorum ($p = 0.002392$). The smaller p shifts the geometric percentile limits toward longer inter-event intervals. Because the geometric distribution is discrete and the control limits are integer-valued, percentile rounding also changes the realized tail probability. Consequently, the realized in-control false-alarm probability for Tokat is lower ($\alpha \approx 0.00238$) than for Amasya ($\alpha \approx 0.00355$) and Çorum ($\alpha \approx 0.00399$), which yields a larger ARL_0 (419.91 versus 281.93 and 250.52, respectively). Thus, the difference is attributable primarily to the province-specific p estimate together with the discrete percentile/rounding structure of the g chart, rather than directly to the number of earthquakes alone. These values describe the nominal behaviour of the selected control-limit design and should not, by themselves, be used to classify individual seismic signals as noise or as physically meaningful anomalies.

4. DISCUSSION

The application domain of the g control chart was extended to natural-disaster monitoring by adapting a rare-event method commonly used for industrial defects or healthcare data to earthquakes exceeding a selected magnitude threshold. This application illustrates how SPC tools can be used in an interdisciplinary event-monitoring context.

Unlike many seismic analyses that focus on the number of earthquakes per unit time, this study focuses on the number of opportunities between successive earthquakes. This perspective addresses limitations that classical count charts (c and u charts) may encounter when seismic datasets contain many zero-event periods and allows unusual changes in event spacing to be examined directly.

The findings show that the wider $k = 3$ limits reduce the number of g control chart signals relative to $k = 1$ and make long event-free intervals and short inter-

event intervals easier to distinguish visually. Nevertheless, neither the $k = 1$ signals nor the $k = 3$ signals were independently validated against an external seismological criterion. In addition, no declustering procedure was applied; therefore, short inter-event intervals and apparent clustering may partly reflect aftershock sequences or other dependent events rather than independent changes in the underlying earthquake-occurrence process. This issue may increase the apparent sensitivity of the g control chart, particularly under the narrower $k = 1$ limits. Accordingly, the observed signals should be treated as statistical indications of unusual event spacing rather than as direct evidence of seismic quiescence, earthquake clustering, stress transfer, triggering, or an impending earthquake. The g control chart may therefore complement, but not replace, established geophysical monitoring and seismic-risk assessment methods. Future research should repeat the analysis using declustered catalogues and compare the resulting signals with those obtained from the complete catalogue.

5. CONCLUSION

The g control chart was applied to earthquakes exceeding the selected magnitude threshold using the "number of opportunities" framework for Amasya, Çorum, and Tokat. The comparison of $k = 1$ and $k = 3$ showed that the selected control-limit width substantially affects the number and visibility of statistical signals. The method can make unusual changes in the spacing between earthquakes visible, but such signals should not be interpreted as proof of non-stationary seismicity, stress transfer, triggering mechanisms, or as a stand-alone earthquake early-warning indicator. Instead, the g control chart should be regarded as a complementary statistical monitoring tool whose signals require evaluation together with seismological and geophysical evidence. The study is limited to three provinces, a single $Mx \geq 4.0$ magnitude threshold, one earthquake catalogue, and the absence of a sensitivity analysis across alternative magnitude thresholds. A further limitation is that the catalogue was not declustered; aftershock sequences and other dependent events may therefore violate the independence assumption of the geometric model and may contribute to short inter-event intervals and clustering-related signals. Future studies should compare complete and declustered catalogues, examine alternative magnitude thresholds, and validate g control chart signals against independent geophysical observations such as GNSS, InSAR, and microseismicity data.

Acknowledgements and Funding

There are no individuals or institutions to acknowledge for this study, and this research received no specific financial support from public, commercial, or not-for-profit funding bodies.

Author Contribution Statement – CRediT

G.S.E.: Conceptualization, Methodology, Investigation, Data curation, Formal analysis, Visualization, Writing - original draft. S.E.: Supervision, Methodology, Writing - review and editing.

Conflict of Interest Statement

The authors declare no competing interests.

Data Availability Statement

The data supporting the findings of this study are available from the corresponding author upon reasonable request.

REFERENCES

[1] Kaminsky, F., Benneyan, J., Davis, R., and Burke, R. (1992). Statistical control charts based on a geometric distribution. Journal of Quality Technology.

[2] Ali, S., Pievatolo, A., and Göb, R. (2016). An overview of control charts for high-quality processes. Quality and Reliability Engineering International, 32(7), 2171–2189. https://doi.org/10.1002/qre.1957

[3] Williams, B., and Ziemnik, L. (2025). Selecting the correct control chart: A practical example from adolescent care. Current Problems in Pediatric and Adolescent Health Care, 55(7). https://doi.org/10.1016/j.cppeds.2025.101805

[4] Sałaciński, T., Chrzanowski, J., and Chmielewski, T. (2023). Statistical process control using control charts with variable parameters. Processes, 11, 2744. https://doi.org/10.3390/pr11092744

[5] Santiago, E., and Smith, J. (2013). Control charts based on the exponential distribution: Adapting runs rules for the t chart. Quality Engineering, 25(2), 85–96. https://doi.org/10.1080/08982112.2012.740646

[6] Benneyan, J. C., Lloyd, R. C., and Plsek, P. E. (2003). Statistical process control as a tool for research and healthcare improvement. Quality and Safety in Health Care, 12(6), 458–464. https://doi.org/10.1136/qhc.12.6.458

[7] Park, C., and Wang, M. (2023). A study on the g and h control charts. Communications in Statistics - Theory and Methods, 52(20), 7334–7349. https://doi.org/10.1080/03610926.2022.2044492

[8] Alexander, M. (2024). Special control charts for rare events: G-charts and T-charts. SESUG Paper, SME-42-2024.

[9] Taskin, F., and Masud, M. S. (2020). Application of statistical control charts to detect unusual frequency of earthquake in the world. Journal of Data Science, 18(1), 44–55. https://doi.org/10.6339/JDS.202001_18(1).0002

[10] Kim, B. R., Chae, B. G., Kim, Y., and Seo, Y. S. (2013). Application of statistical analysis to analyze the spatial distribution of earthquake-induced strain data. The Journal of Engineering Geology, 23(4), 353–361. https://doi.org/10.9720/kseg.2013.4.353

[11] Yücemen, S. (2013). Estimation of seismic hazard: Probabilistic and statistical methods. TÜİK İstatistik Araştırma Dergisi, Özel Sayı 2013.

[12] Amei, A., Fu, W., and Ho, C. H. (2012). Time series analysis for predicting the occurrences of large scale earthquakes. International Journal of Applied Science and Technology.
[13] Reasenberg, P. A., and Matthews, M. V. (1988). Precursory seismic quiescence: A preliminary assessment of the hypothesis. Pure and Applied Geophysics, 126(2–4), 373–406. DOI: 10.1007/BF00879004.
[14] Benneyan, J. C. (2001). Performance of number-between g-type statistical control charts for monitoring adverse events. Health Care Management Science, 4(4), 319–336. https://doi.org/10.1023/A:1011806727354
[15] Minitab, LLC. (2026). Methods and formulas for G chart. Minitab Support. Retrieved August 9, 2026, from https://support.minitab.com/en-us/minitab/help-and-how-to/quality-and-process-improvement/control-charts/how-to/rare-event-charts/g-chart/methods-and-formulas/methods-and-formulas/
[16] Karakus, Z. (2013). Performance comparison of statistical process control methods to monitor grouped data and rare events in healthcare applications.
[17] Torng, C. C., and Lee, P. H. (2008). ARL performance of the Tukey's control chart. Communications in Statistics - Simulation and Computation, 37(9), 1904–1913. https://doi.org/10.1080/03610910802263141
[18] General Directorate of Mineral Research and Exploration. (2026). Geosciences map viewer. April 16, 2026, Retrieved from https://yerbilimleri.mta.gov.tr/anasayfa.aspx
[19] Boğaziçi University Kandilli Observatory and Earthquake Research Institute. (2026). Numerical data. April 16, 2026, Retrieved from http://www.koeri.boun.edu.tr/sismo/2/deprem-verileri/sayisal-veriler/